

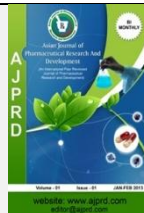
Available online on 15.04.2020 at <http://ajprd.com>



**Asian Journal of Pharmaceutical Research and Development**

Open Access to Pharmaceutical and Medical Research

© 2013-20, publisher and licensee AJPRD, This is an Open Access article which permits unrestricted non-commercial use, provided the original work is properly cited



Open  Access

Review Article

## Mesoporous Silica Nanoparticles Based Antigens and Nucleic Acids Delivery: A Review

Jemal Dilebo

Department of Pharmaceutics and Social Pharmacy, School of Pharmacy, College of Health Sciences, Addis Ababa University, Ethiopia

### ABSTRACT

Mesoporous silica nanoparticles (MSN) have been explored for the delivery of small molecule drugs, antigens, and nucleic acids because of their large surface area, pore volume, amenability of their surface for functionalization, stable mesoporous structure, and biocompatibility. Biomolecules loading capacities, release and target cell accumulation efficiencies have been improved for both antigen and nucleic acid delivery by the synthesis of large-pore MSN, dendritic MSN, hollow-core MSN, and multifunctional MSN. This article overview the major advances in the use of MSN for delivery of antigens and therapeutic nucleic acids such as DNA, siRNA, and miRNA aimed for treatment of various diseases.

**Key words:** Mesoporous silica nanoparticles, antigen, adjuvant, DNA, siRNA, miRNA

**ARTICLE INFO:** Received 18 Jan. 2019; Review Completed 6 March 2020; Accepted 27 March 2020; Available online 15 April. 2020



#### Cite this article as:

Dilebo J, Mesoporous Silica Nanoparticles Based Antigens and Nucleic Acids Delivery: A Review, Asian Journal of Pharmaceutical Research and Development. 2020; 8(2):50-57. DOI: <http://dx.doi.org/10.22270/ajprd.v8i1.686>

#### \*Address for Correspondence:

Jemal Dilebo, Department of Pharmaceutics and Social Pharmacy, School of Pharmacy, College of Health Sciences, Addis Ababa University, Ethiopia.

### INTRODUCTION

There are different types of mesoporous silica nanoparticles (MSN) which mainly differ in the geometry of their mesostructures. The first types of these novel materials have been given the name M41S and includes MCM-41, MCM-48, and MCM-50. MCM-41 (Mobil Crystalline Material) is the first type of mesoporous material synthesized by Mobil corporation in 1992<sup>1</sup>. Other types of MSN are known as SBA-15 and SBA-16 (Santa Barbara Amorphous type materials). SBA-15 has a 2D hexagonal mesostructure and prepared under acidic conditions using triblock copolymers and SBA-16 possesses 3D cubic arrangement corresponding to Im3m space group<sup>2-3</sup>. SBA type of mesoporous materials have pore diameter in the range of 20 and 300 Å, which is larger than M41S type of mesoporous materials<sup>2</sup>. Possession of large mesoporous pores (2-50 nm), surface areas and suitability of their surface for modifications makes them suitable for delivery of therapeutic biomolecules such as antigens and nucleic acids. Apart from drug loading function MSN are utilized in different field for application in catalysis, separation and sorption<sup>4</sup>.

### Antigen Delivery and adjuvant potential of MSN

#### Conventional MSN

A study by Mahony et al<sup>5</sup> showed that amine functionalized MSN had more ovalbumin loading capacity than unfunctionalized MSN. The electrostatic attraction between positive charge of amine and negatively charged amino acids in the ovalbumin is responsible for enhanced loading capacity of MSN<sup>5</sup>.

Aqueous dispersity and stability of boron nitride nanospheres (BNNS) was enhanced when the surface was encased with MSN<sup>6</sup>. The hybrid of BNNS and MSNs and amine surface functionalized nanovector called BNNS@MS-NH<sub>2</sub> and loaded with CpG oligodeoxynucleotides (CpG ODNs) induced much higher amounts of IL-6, IFN- $\alpha$ , and TNF- $\alpha$  from murine RAW 264.7 macrophages due to significantly enhanced cellular uptake of BNNS@MS-NH<sub>2</sub>. Whereas free CpG ODNs stimulated very small amounts of cytokine secretion. In addition, BNNS@MS-NH<sub>2</sub> showed the highest anti-proliferative effect on murine mammary tumor cells (4T1) cells.

The effect of surface chemistry of MSN on vaccine delivery was evaluated<sup>7</sup>. OVA loaded in mesoporous silica nanorods (MSNRs) surface modified with hydrophobic group (C<sub>18</sub>) induced effective expression of costimulatory molecules, high secretion of IFN- $\gamma$ , highest antigen-specific splenocyte proliferation and IgG response compared to nanorods surface modified with hydroxyl or amine groups<sup>7</sup>. Moreover, MSNRs surface conjugated with C<sub>18</sub> promoted a switch from Th2 to Th1 immune response. One factor for the highest immunogenicity of MSNRs-C<sub>18</sub>/OVA could be the high load of OVA carried in these nanoparticles than OH or NH<sub>2</sub> modified MSNRs. In addition, OVA release from MSNRs-C<sub>18</sub>/OVA and MSNRs-NH<sub>2</sub>/OVA was sustained and contributed for the enhanced immunogenicity compared with the MSNRs-OH/OVA from which antigen was released in rapid manner.

Synergistic effect between large pore (35 nm) stellated fibrous spherical mesoporous silica nanospheres and polyinosinic-polycytidylic acid (Poly (I:C) against E.G7-OVA tumor was observed<sup>8</sup>. The combination of stellated fibrous MS nanospheres with poly(I:C) significantly decreased the necessary dose of poly(I:C) for anti-tumor immunity. Mice immunized with MS-OVA-PIC had significantly higher anti-cancer immunity than those without immunization or immunized with OVA-PIC (at same poly(I:C) dose of 0.625 mg/kg). In addition, mice immunized with MS-OVA-PIC at poly(I:C) dose of 0.625 mg/kg showed comparable anti-cancer immunity to those immunized with 2.5 mg/kg of free poly(I:C). The reduced dose of poly (I:C) used in this study can reduce the side effects associated with the use high dose of poly(I:C).

#### Large pore MSN

Double-stranded DNA (dsDNA) with 72 bp was bound successfully with amine modified MSN<sup>9</sup>. The binding of dsDNA with the modified MSN improved serum stability of dsDNA and was highly up taken by murine macrophages. High loading efficiency of dsDNA was achieved as the MSN had mean pore size of about 11 nm. At loading ratio of MSN-NH<sub>2</sub>: dsDNA of 3, 184  $\mu\text{g mg}^{-1}$  of dsDNA was achieved which was much higher than those of solid silica nanoparticles (6.7  $\mu\text{g mg}^{-1}$ ) and MCM-41 with a mesopore size of 2.5 nm (38.8  $\mu\text{g mg}^{-1}$ ). Stability study in serum-containing medium indicated that MSN-NH<sub>2</sub>/dsDNA complexes were able to protect dsDNA against degradation by nuclease. MSN-NH<sub>2</sub>-dsDNA complexes induced high levels of IFN- $\alpha$  than DOTAP liposomal transfection reagent (79.1  $\text{pg ml}^{-1}$  vs 66.2  $\text{pg ml}^{-1}$ ).

Cha et al.<sup>10</sup> synthesized amine modified MSN with extremely large pore MSN (XL-MSN) with pore size of about 25 nm and successfully loaded simultaneously with ovalbumin, CpG oligodeoxynucleotide, and toll-like receptor-9 agonist as cancer vaccine. When the nanocarrier was subcutaneously injected in left flank and footpad of mice, it travelled to the nearby lymph node. The better nanoparticles are taken up by APCs and the deeper trafficking to lymph nodes, the greater will be the immune response (Du et al., 2017). Mice immunized with XL-MSN co-loaded with OVA and CpG had significantly inhibited tumor growth and the highest survival compared with other groups<sup>10</sup>.

Kwon et al.<sup>11</sup> synthesized XL-MSN with pore size of 30 nm using CTAB stabilized iron oxide nanoparticles as seed

material. The XL-MSN was successfully loaded with chicken ovalbumin (MW 43 kDa), bovine serum albumin (MW 66 kDa), and glucose oxidase (MW 160 kDa) 3.5, 9.3, and 6.2 fold higher, respectively, than conventional MSNs (pore size of 3.2 nm). When loaded with IL-4, M2 macrophage polarization (anti-inflammatory macrophages) was induced both in *in vitro* and *in vivo*. XL-MSN had dose and time dependent toxicity to murine macrophage and induced less production of ROS.

Extra-large pore mesoporous silica nanoparticles (XL-MSN) (mesopore size 20-30 nm) decorated with small gold nanoparticles (AuNPs) and conjugated with PEG were synthesized using iron oxide nanoparticles as seed material for delivery of thiolated CpG oligodeoxynucleotides (SH-CpG-ODNs) (Au@XL-MSNs-CpG-PEG)<sup>12</sup>. High amount of SH-CpG-ODN per XL-MSN was loaded (i.e., 160 $\mu\text{g}$  SH-CpG-ODN/mgXL-MSNs). The release pattern of SH-CpG-ODNs *in vitro* was initially burst release followed by sustained release in later times. The slow release of CpG-ODNs was due to more robust gold-thiol bonding in Au@XL-MSNs-CpG. Au@XL-MSNs-CpG-PEG caused the highest activation of bone marrow derived dendritic cells compared to soluble CpG. Intratumoral injection of Au@XL-MSNs-CpG-PEG along with near infrared laser radiation (NIR) into 4T1 showed a synergetic effect in tumor growth inhibition compared to the nanocarrier without NIR irradiation. When NIR irradiation is applied to tumor cells, the generated heat destroys tumor cells and the dead cells will release tumor antigens which can be taken up by tumor residing DCs along with the nanocarriers. The DCs will be highly activated and thereby enhance antigen presentation<sup>12</sup>.

#### Hollow mesoporous silica nanoparticle (HMSNs)

Hollow mesoporous silica nanospheres (HMS) with pore size range 2-6 nm was synthesized<sup>13</sup>. HMSNs was formed from non-hollow mesoporous silica nanospheres (MS) by increasing incubation temperature from 25 °C to 70 °C<sup>13</sup>. The formation of hollow space in the inner section could be due to lower degree of silica condensation in the inner section than outer layer which could be preferentially dissolved when incubation temperature is elevated<sup>14</sup>. Mice immunized with HMS co-loaded with OVA and a synthetic analog of double-stranded RNA (poly IC) had cancer size of 338 mm<sup>3</sup>; whereas the group administered with MS-OVA-Poly IC had cancer size of about 846 mm<sup>3</sup> one month after E.G7-OVA challenge. But mice immunized with saline-OVA had cancer size of about 5121 mm<sup>3</sup> at the endpoint.

Xie et al.<sup>15</sup> synthesized hollow mesoporous silica nanoparticles to load two melanoma derived antigenic peptides (HGP100<sub>25-33</sub> (H) and TRP2<sub>180-188</sub> (T)) with different hydrophobicities to evaluate prophylactic and anti-metastatic effects in mice against B16-F10 melanoma cells. The surface of the nanoparticles was coated with monophosphoryl lipid A (MPLA) containing lipid bilayer and the formed nanoparticle was called HTM@HMLBs to improve the stability and biocompatibility of HMSNs. Mice administered with HTM@HMLBs had delayed tumor occurrence, significantly smaller tumor volume, tumor weight, and lower lung metastatic nodules. Coating MSN surface have been shown to improve colloidal stability and prolonged the release of antigens as the coat acts as a gate at the pore opening<sup>16</sup>.

Biodegradable lipid layer coated hollow mesoporous silica nanoparticles (dHMLB) with hollow core size 70 nm and mesopores was synthesized for co-delivery of doxorubicin (DOX), all-trans retinoic acid (ATRA) and interleukin-2 (IL-2) to achieve enhanced antitumor efficiency by Kong et al.<sup>17</sup>. In order to form hollow structure core selective etching using Na<sub>2</sub>CO<sub>3</sub> was employed. Antitumor activities of the dHMLB formulations were tested against mice tumor model B16F10. A/D/I-dHMLB exhibited much higher tumor inhibitory rate (84.8%) and lesser number of metastatic nodules (60) in the lung of mice compared to other formulations. The result demonstrated that co-loading of tumor microenvironment modulator, chemotherapeutic and immune agent could achieve better synergistic effects in inhibiting tumor growth compared with any of two therapeutic agents co-loaded in dHMLB.

#### **Dendritic mesoporous silica nanoparticles (DMSN)**

Lu et al.<sup>18</sup> synthesized PEI modified GSH-depletion dendritic mesoporous organosilica nanoparticles (GDMON-P) with tetra-sulfide bond embedded in the MSN framework and loaded with OVA and CpG oligodeoxynucleotide for cancer immunotherapy. The particle and pore sizes were 400 nm and 22.7 nm, respectively. In mice bearing B16-OVA tumor, GDMON-P loaded with OVA and CpG exhibited improved anti-tumour performance than OVA and CpG loaded in non-GSH-depletion dendritic mesoporous organosilica nanoparticles (NDMON) or other formulations. The improved antitumor performance of GDMON-P based formulation could be due to three aspects. Firstly, depletion of intracellular GSH induces high level of ROS which results in enhanced maturation of APCs. Secondly, GSH dependent degradability of GDMON-P enables antigen release inside APCs. Thirdly, PEI conjugated GDMON deliver antigens in the cytosol and favors MHC-I presentation for further activation of CD8<sup>+</sup>T cells<sup>18</sup>.

Abbaraju et al.<sup>19</sup> synthesized DMSN with solid silica-fullerene core and dendritic silica shell with large pores (28 nm) to simultaneously deliver photosensitizer and monoclonal antibody for photodynamic therapy and immunotherapy. Fullerene (C<sub>60</sub>) doped in silica serves as photosensitizer and fluorescent agent for imaging. Dendritic shell modified with octadecyl enabled the successful loading of anti-pAkt mAb. Better MCF-7 cell inhibition was found at longer UV illumination, higher nanoparticle concentration and UV light along with anti-pAkt.

Abbaraju et al.<sup>20</sup> also synthesized unique asymmetric head-tail MSN (HTMSN). The asymmetric HTMSN has numerous dendritic tails with large pores (11-28 nm) budded on solid or porous spherical silica head. The dendritic tail length and surface converge was tailor made. The asymmetric HTMSN were better up taken by APC and more hemocompatible for RBC compared to stober spheres, conventional MSN, and HTMSN with full dendritic surface coverage. The head-tail morphology of asymmetric HTMSN attributed better phagocytosis and induced better *in vitro* APCs maturation when loaded with OVA than the symmetric ones. In addition, asymmetric HTMSN showed balanced efficacy and safety of adjuvant activity than alum and have a great potential in therapeutic cancer vaccines in which alum is less effective.

Yang et al.<sup>21</sup> demonstrated organosilica framework structure and the architecture of MSN affected anticancer immune response. Double-shelled dendritic mesoporous organosilica hollow spheres (DMOHS-2S) were found to be excellent adjuvants and provided greater immunity than double-shelled dendritic mesoporous silica hollow spheres (DMSHS-2S) or single-shelled dendritic mesoporous organosilica hollow spheres (DMOHS-1S). When evaluated for immunopotentiating effect, DMOHS-2S loaded with B16F10 tumor cell fragments (TF) induced the highest amount of CD4<sup>+</sup> and CD8<sup>+</sup> T cells compared to other formulations; indicating higher potential for stimulating humoral and cell mediated immunity. Moreover, mice immunized with DMOHS-2S+TF exhibited a 50% survival rate after 35 days of tumor inoculation. In addition, mice immunized with DMOHS-2S+TF vaccine formulation had prolonged tumor free rate and up to 31 days delay in tumor growth; whereas the remaining groups had a 100% tumor occurrence within 25 days. The authors concluded that both the organosilica rich composition and the double-shelled structure are favorable for the enhanced adjuvant effect *in vivo*.

#### **Adjuvant potential of conventional MSN**

Antigen loaded MSN can elicit immune response at reduced antigen dose compared to a conventional delivery system<sup>16</sup>. For example, subcutaneous immunization with 2 µg of OVA-loaded MSNs induced comparable antibody responses as 50 µg OVA adjuvanted with Quil-A<sup>5</sup>. One of the reasons for immune enhancing effect of MSN may be the increased uptake by dendritic cells when OVA is associated with MSNs.

The adjuvant potential of SBA-15 and SBA-16 in mice with a recombinant HSP70 surface polypeptide domain (HSP70<sub>212-600</sub>) from *Mycoplasma hyopneumoniae* was assessed<sup>22</sup>. The antigen combined with SBA-15 elicited high serum total IgG level comparable to the antigen combined with alum. SBA-15 along with the antigen induced increased levels of IFN-γ, IL-4 and IL-10. On the other hand SBA-16 along with the antigen induced lower levels of total IgG and no induction of cytokine release from splenocytes-derived dendritic cells.

In a study by Wang et al.<sup>23</sup>, *ex vivo* production of INF-γ, IL-2, IL-4, IL-10 induced by MSN plus OVA was higher compared with Alum plus OVA in mice when lymph node drained lymphocytes were stimulated for three days with 0-100 µg/ml OVA. Moreover after three months of adjuvant injection, the population of CD4<sup>+</sup> and CD8<sup>+</sup> T cell in bone marrow, lymph node, and spleen were enhanced as compared with those immunized by alum and adjuvant-free groups. In addition, MSN-OVA immunized mice showed significantly improved OVA-specific IgA, IgG2a, IgG, and IgG1 titers as compared with those immunized with alum-OVA or saline-OVA groups at day 28 and 38<sup>23</sup>.

Wang et al.<sup>24</sup> synthesized biodegradable monodispersed mesoporous silica nanospheres (MS) doped with calcium, magnesium, and zinc for cancer immunotherapy. The degradation rate of MS, MS-Ca, MS-Mg and MS-Zn *in vivo* one day after subcutaneous injection was 24%, 50.8%, 52.8% and 56.3%, respectively.

Mice immunized with MS-OVA, MS-Ca-OVA, MS-Mg-OVA and MS-Zn-OVA had greatly inhibited cancer volume. Moreover, MS-OVA, MS-Ca-OVA, MS-Mg-OVA

and MS-Zn-OVA nanospheres administered mice had significantly increased population of CD4+ and CD8+ T cells compared with those without immunization. Among all the groups, mice immunized with MS-Zn-OVA had the highest percentages of CD4+ and CD8+ T cells in their lymphocytes. In addition, MS-OVA, MS-Ca-OVA, MS-Mg-OVA and MS-Zn-OVA-treated mice exhibited significantly higher cytokines secretion including Th1-type IFN- $\gamma$  and Th2-type IL-4. The MS-Zn-OVA-administrated mice had the highest OVA-specific IFN- $\gamma$  secretion by lymphocytes in *ex vivo* among all the groups. The highest anti-cancer Th1 immunity of MS-Zn nanospheres may be due to the synergistic effect of Zn and MS.

#### Adjuvant potential of hollow MSN (HMSN)

Mahony et al.<sup>25</sup> was able to load 500  $\mu$ g E2 protein from Bovine viral diarrhoea virus 1 (BVDV-1) on to 6.2 mg amine functionalized HMSN (HMSA) to stimulate immune response in sheep. The antigen loaded HMSA was formulated either in freeze-dried or non-freeze dried form. The level of the antibody responses detected to both non-freeze-dried and freeze-dried nanoformulations were similar to those obtained for E2 plus Quil-A (saponin from *Quillaja saponira*). On the other hand the freeze-dried formulation elicited more cell mediated immunity response than E2 plus Quil-A or non-freeze-dried formulation four months after the last immunization. This study also confirmed vehicle and adjuvant potential of HMSN.

In a study by Bai et al.<sup>26</sup> spherical hollow mesoporous silica nanoparticles (HMSN) with average particle size of 400 nm and mesopore size of approximately 2.2 nm adsorbing foot-and-mouth disease virus like particle (VLP) (HMSNs/VLPs) administered into guinea pigs elicited stronger and more persistent immunity compared with Freund's complete adjuvant/VLP. The levels of specific antibodies of guinea pigs immunized with HMSNs/VLPs or VLPs/Freund's complete adjuvant showed similar trend; greatly increased at the 4<sup>th</sup> week and reached the peak at the 10<sup>th</sup> week and then decreased significantly. However, the antibody titers of the group vaccinated with the HMSNs/VLPs were significantly higher than those of the VLPs/Freund's complete adjuvant at the 14<sup>th</sup> week. T-lymphocytes proliferation was more evident in the group immunized with HMSNs/VLPs than in the group immunized with VLPs/Freund's complete adjuvant. On protective test against foot-and-mouth disease virus, all the guinea pigs were infected in the groups immunized with PBS, HMSN, or blank control. But the protection rates of groups immunized with HMSNs/VLPs or VLPs/Freund's complete adjuvant were 80%. Moreover, up to 50% of VLP was released at day 9 indicating sustained release of VLP.

#### Adjuvant potential of large-pore MSN

Large-pore mesoporous-silica-coated  $\beta$ -NaYF<sub>4</sub>:20% Yb, 2%Er upconversion nanoparticles (UCMSs) with size less than 100 nm and pore size >30 nm were prepared as novel immunoadjuvant against CT26-tumor in mice<sup>27</sup>. The UCMSs were successfully co-loaded with photosensitizer merocyanine 540 (MC540), chicken ovalbumin (OVA), and tumor cell fragment (TF). When CT26-tumor-bearing mice were subcutaneously immunized with different formulations, the group administered with UCMSs-MC540-OVA + laser (980 nm NIR laser with a power density of 0.5 W cm<sup>-2</sup> for 10 min), produced significantly greater secretion of IFN- $\gamma$ , IL-12, and TNF- $\alpha$  relative to

other groups indicating strong Th1 immune response. Additionally, this group produced the highest secretion of IL-4 indicating strongest Th2 immune response. When investigating the immunoadjuvant potential of UCMSs-MC540-TF + laser in tumor volume of 100 mm<sup>3</sup>, the tumor dramatically regressed starting at day 10 and some tumors even disappeared after 18 days of treatment and the group survived over 65 days which was significantly more than any other group.

#### Adjuvant potential of hollow core MSN (HMSN)

Peng et al.<sup>28</sup> evaluated vaccine carrier/adjuvant potential of HMSN with particle size of 100 nm and mesopore size of 2.897 nm loaded with house dust mite antigen (Derf2 protein). High antigen loading capacity was achieved (90  $\mu$ g Der f2 / 1 mg HMSNs). Der f2 was released initially fast and then sustained in which 10.8% and 14.5 % Der f2 was released after 24 hr and 72 hr, respectively. In allergic model of mice, Der f2 loaded in HMSNs (Der f2-HMSNs) treated mice had lower level of Der f2 sIgE, IL-4, WBC number, and eosinophils percentage than Der f2/Al(OH)<sub>3</sub> treated group. Moreover, Der f2-HMSNs treated mice had higher level of Der f2 sIgG and IFN- $\gamma$  than Der f2/Al(OH)<sub>3</sub> treated group. The authors stated that the relatively higher anti-allergic effect of Der f2-HMSNs could be attributed to small particle size, spherical shape and slow release of Derf2 protein from the cargo.

#### Nucleic acid delivery

##### Surface-positively charged MSN

MSN surface modified with PEI and co-loaded with DOX and multidrug resistant protein 1 siRNA (MDR1 siRNA) to block gene expression of MDR1 in cancer cells was synthesized<sup>29</sup>. Therapeutic effect of DOX and MDR1 siRNA co-loaded MSN-PEI was evaluated in mice bearing human oral squamous carcinoma DOX-resistant cell line (KBV cells) by intratumoral injection once a day for 5 days. At 28 days of post-treatment, tumor growth rates and sizes were not significantly different between negative control and MSNP-PEI/MDR1-siRNA groups. Tumor growth rates and sizes from MSNP-PEI-DOX and MSNP-PEI-DOX/MDR1-siRNA treated groups were, however, significantly different from the control and MSNP-PEI/MDR1-siRNA groups at 28 days post-treatment. The results imply that MSNP-PEI-DOX/MDR1-siRNA can enhance the killing effect of DOX through the inhibition of MDR1 gene expression.

In order to enhance gene transfection efficiency and reduce cytotoxicity of PEI functionalized MSN, Zhan et al.<sup>30</sup> functionalized HMSN with PEI with molecular weight of 1.8 kD. They were also able to functionalize the inner wall of HMSN with PEI to enhance DNA adsorption. As the result the resulting PEI-HMSN was able to load up to 37.98 mg green fluorescent protein (GFP) labeled DNA per g of HMSN. At PEI-HMSN to DNA ratio of 60, *in vitro* transfection efficiency of PEI-HMSN loaded with DNA into human colonic carcinoma cell line Lovo was 48.06%. The transfection efficiencies of naked GFP-DNA, DNA-1.8KD PEI, DNA-25 KD PEI, were 2.30%, 1.67%, and 21.89%, respectively.

Positively charged fluorescent mesoporous silica nanoparticle (FMSN+) was used to co-deliver Nurr1 plasmid (pNurr1) and Rex1 siRNA (siRex1) into induced pluripotent stem cells (iPSCs) to achieve dopaminergic

neuron differentiation<sup>31</sup>. On cytotoxicity study, pNurr1-siRex1-FMSN(+) caused 12% and 30% cell deaths at 96<sup>th</sup> hr and 14<sup>th</sup> day, respectively. Whereas transfection with lipofectamine 2000 (Lipo) caused 43% and 70% cell deaths, respectively in the stated times. In the determination of mRNA-expression levels for neuron genes, 60 hr after transfection, the expression levels of Rex1 and pluripotency marker were reduced by 98% when treated with pNurr1-siRex1-FMSN(+) compared to the control condition which indicated that pNurr1-siRex1-FMSN(+) delivery caused the down regulation of the expression of Rex1 mRNA, which demonstrated that siRex1 was successfully transfected by FMSN(+). Moreover, pNurr1-siRex1-FMSN (+) mediated delivery was more effective than pNurr1-siRex1-Lipo (positive control) in knockdown of Rex1. FMSN+ were also effective in the transfection of Nurr1 and synergistically improved expression of the neuron-associated genes. Also the percentage of dopaminergic markers like Th (tyrosine hydroxylase, a dopamine-related enzyme) and Dat (dopamine transporter, a symporter that moves dopamine across the cell membrane) were evaluated at day 7 and 14. At day 7, iPSCs transfected with pNurr1-siRex1-FMSN(+) produced 83.0% of Th-expressing cells and 65.2% of Dat-expressing cells. Whereas the untreated cells showed only 52.2% of Th-expressing cells and 43.6% of Dat-expressing cells. At day 14, cells treated with pNurr1-siRex1-FMSN(+) produced 89.9% Th-expressing cells and 88.5% Dat-expressing cells. Whereas the untreated cells had 51.4% Th-expressing cells and 49.3% Dat-expressing cells. The amount of dopamine released from neuron-like cells that were differentiated from iPSCs after transfection with pNurr1-siRex1-FMSN(+) was 5 ng/mL at Day 7 and 12.5 ng/mL at day 14. Whereas the positive control secreted 2.5 ng/mL and 8 ng/mL at day 7 and 14, respectively.

Gene transfecting efficacies of MCM-41 (MCM-41-OH), MCM-41-NH<sub>2</sub>, MCM-41-imidazole (MCM-41-Im) loaded with pDNA was assessed in HeLa cells *in vitro*<sup>32</sup>. The interaction between the nanocarriers and pDNA was assessed and found that MCM-4-NH<sub>2</sub> had a weak interaction with pDNA than MCM-41-Im at similar molar ratio of amine group to DNA phosphate groups (N/P). The expression level of EGFP plasmid was significantly higher for the MCM-41-Im than MCM-41-NH<sub>2</sub>. In addition, compared to the Metafectene® (standard transfecting agent), MCM-41-Im showed a higher level of gene expression (~95%) at N/P = 1 which could be attributed to enhanced cellular uptake and/or endosomal escape caused by imidazole group<sup>32</sup>.

Chen et al.<sup>33</sup> prepared amine functionalized and Epidermal Growth Factor (EGF) grafted rod shaped MSN with aspect ratio of 1, 1.5 and 2.5. Among them, MSN-1.5 had the highest loading efficiency for siRNA which was about 80.53 mg/g. Transfection efficiency was evaluated in colorectal cancer cell line SW480 which over expresses Epidermal Growth Factor Receptor (EGFR). The cellular uptake rate and mean fluorescent intensity (MFI) of cells transfected with siRNA loaded in EGF-MSNs-1.5 were found to be much higher than cells treated with Lipofectamine 2000 or MSNs-1.5 without EGF. When studying gene silencing capacities of survivin siRNA loaded in MSN-1.5-EGF, gene expression of cells transfected with MSNs-1.5-siRNA and EGF-MSNs-1.5-

siRNA was decreased nearly to 60% and less than 30%, respectively.

MSN with large and small mesopores (H-MSN) existing in separate parts of the matrix was fabricated to sequentially release siRNA and DOX (the initial inhibition of pg-1 expression and subsequent therapeutic effect of DOX) in DOX-resistant MCF-7 cell lines (MCF-7/ADR)<sup>34</sup>. The small mesopores were located in the silica core and the larger mesopores located within the organosilica shell with integrated disulfide bonds. In the synthesis of H-MSN, mixture of tetraethyl orthosilicate and bis[3-(triethoxysilyl)propyl]tetrasulfide (BTES) was added drop wise to the MSN reaction solution (before the centrifugation step) and the mixture was stirred for few hours, collected, washed and extracted in the usual MSN fabrication way and the synthesized MSN was designated as MSNs@MONs. After a number of reaction steps, MSNs@MONs surface was finally grafted with PEI. In order to evaluate antitumor effect of the nanocarrier against MCF-7/ADR tumor model, tumor volume of about 150 cm<sup>3</sup> was generated in mice and the nanoformulations and controls such as PBS, H-MSNs-siRNA, free DOX, H-MSNs-DOX and H-MSNs-DOX/siRNA were administered into the tumor at DOX concentration of 5 mg/kg. In mice administered with H-MSNs-DOX/siRNA, tumor inhibition rate was 87%. Mice in the groups of H-MSNs-DOX had 76.8% inhibition rate and free DOX group had 50.7% inhibition rate. The authors stated that in mice treated with H-MSNs-DOX/siRNA, P-gp was significantly down-regulated as compared to H-MSNs-DOX treated group because of the siRNA-silencing effect which strongly implies H-MSNs-DOX/siRNA can reverse the MDR of cancer cells through down-regulating P-gp expression.

Co-delivery of carfilzomib (a proteasome inhibitor) with anticancer drugs (etoposide and docetaxel) and survivin siRNA in PEI conjugated MSNs showed higher gene silencing effect compared to MSN co-loaded with both drugs or combined free drugs in malignant A549 cells<sup>35</sup>.

Low molecular weight PEI was electrostatically adsorbed on the surface of monodispersed MSN for delivering anti-TWIST siRNA to Epithelial Ovarian Cancer<sup>36</sup>. TWIST is epithelial-to-mesenchymal transition (EMT) marker which plays an essential role in cancer metastasis<sup>37-38</sup>. When compared to third generation dendrimer, MSN required extended incubation time for transfecting A2780R and Ovar8 cancer cell lines *in vitro* but MSN knockdown lasted longer. When mice were administered weekly for four weeks MSN-siTWIST, MSN-siQ (negative control), MSN-siQ+ cisplatin, and MSN-siTWIST + cisplatin (combination), at the end of four weeks treatment, mice administered with MSN-siQ had significantly developed tumors and produced disseminated masses. The MSN-siTWIST treatment group produced relatively smaller tumors, with a 30% drop in bioluminescent signal at the end of therapy in comparison to the controls. The treatment group with MSN-siQ and cisplatin had a tumor burden reduction rate of about 50%, whereas the MSN-siTWIST + cisplatin had an almost 85% decrease. But mice treated with MSN-siTWIST twice weekly at half dose failed to show such differences.

In another study MSN surface conjugated with  $\beta$ -cyclodextrin-grafted PEI (CP) and loaded with DOX and siRNA against pyruvate kinase M2 (PKM2) (a key gene

over expressed in most breast cancer cells) was synthesized<sup>39</sup>. DOX was loaded both in the mesopores of MSN and hydrophobic cavities of cyclodextrin (CD) and siRNA was electrostatically adsorbed with CP on the surface. In vitro transfecting efficacy was evaluated in MDA-MB-231 breast cancer cells and the result was CP-MSN@DOX caused a ~30% reduction in cell viability, while the corresponding value for CP-MSN@DOX/PKM2 siRNA was ~80%. The authors stated that PKM2 siRNA sensitized cells to DOX.

When mice were IV injected once a week for four weeks with PBS, CP-MSN, CP-MSN@DOX, CP-MSN@DOX/ScrsiRNA, or CP-MSN@DOX/PKM2 siRNA, the volume of tumor at the end of therapy was about 1,200 mm<sup>3</sup>, 1,100 mm<sup>3</sup>, 950 mm<sup>3</sup>, 950 mm<sup>3</sup>, and 400 mm<sup>3</sup>, respectively. Whereas the relative weight of tumor with respect to PBS treated group was about 100%, 100%, 70%, 75%, 30%, respectively.

Amine functionalized MSN and loaded with anti-miR-155 and surface covered with polymerized dopamine and then covalently conjugated with AS1411 aptamer (MSNs-anti-miR-155@PDA-Apt) was synthesized for antitumor effect against drug sensitive and resistant human colorectal cancer cell lines (SW480)<sup>40</sup>.

The MSNs-anti-miR-155@PDA-Apt was evaluated for its efficiency to silence the expression of MicroRNA-155 (miR-155) and nuclear factor kappa B (NF-κB). MicroRNA-155 (miR-155) is one of the most salient oncogenic microRNA (oncomiR), which is upregulated in many human cancers such as colorectal cancer (CRC)<sup>41</sup>. Nuclear factor kappa B (NF-κB) is an important transcription factor that regulates the expression of target genes involved in cell growth, apoptosis, angiogenesis, immune and inflammatory response and plays an important role in the process of tumor development and progression<sup>42-43</sup>. When evaluated for antitumor effect in SW480 xenografted mice, the average weight of tumor at 14<sup>th</sup> day was about 200 mg and 300 mg in mice administered with MSNs-anti-miR-155@PDA-Apt + 5-Fluorouracil (5-FU) and MSNs-anti-miR-155@PDA-Apt, respectively. Whereas the weight of tumor in mice administered with normal saline (control group) was about 550 mg. Moreover, administration of MSNs-anti-miR-155@PDA-Apt was found to increase the sensitivity of multidrug resistant SW480 cells towards 5-FU.

Redox stimuli-responsive MSN attached with poly(amidoamine) dendronized chitosan derivative (CP) through disulfide linker was synthesized for co-delivery of DOX and p53 plasmid to Hela cells<sup>44</sup>. Such nanocarriers were represented as MSN-SS-CP and the average particle size of MSN-SS-CP was about 110 nm. Chitosan polymer could be shed from the particle surface triggered by glutathione (GSH) and then the encapsulated DOX will follow. The p53 plasmid is adsorbed on the surface of MSN-SS-SP as the surface carries positive charge. When investigating the apoptosis potential of DOX and p53 plasmid loaded cargoes in Hela cells, the *in vitro* apoptosis for MSN-SS-CP/p53 (w/w = 80:1, p53 = 2 μg/well) and MSN-SS-CP/DOX (DOX = 2 μg/well) were nearly 15% and 25%, respectively. Whereas for MSN-SS-CP/p53/DOX (p53 = 2 μg/well, DOX = 2 μg/well) it was 42.1% indicating the synergistic effect of DOX and p53 in cancer cell apoptosis.

### Dendritic mesoporous silica nanoparticles (DMSN)

Wang et al.<sup>45</sup> synthesized PEI functionalized DMSN with small particle size (50 nm) and dendritic pore size (> 20 nm) at room temperature using a facile method. DMSN with small particle and large pore demonstrated higher *in vitro* mRNA transfection efficiency than MSN with similar particle size and small pore size or DMSN with similar pore size and large particle size

In another study Schiff-base linked imidazole dendritic mesoporous silica nanoparticle (SL-iDMSN) with particle size of 140–200 nm and pore size of about 9.3 nm were synthesized in three step process for loading DOX and iSur-pDNA to release the cargos at acidic endosomal conditions against hepatoma tumor<sup>46</sup>. Drug loading and encapsulation efficiencies for SL-iDMSN were 21.2% and 77.6%, respectively. For DMSN it was 22.6% and 84.3%, respectively. When evaluating for gene silencing efficiency by using real time PCR for SL-iDMSN and DMSN loaded with iSur-pDNA, the % of cell expressed survivin mRNA were about 50% and 82.5%, respectively. DOX and iSur-pDNA co-loaded SL-iDMSN and DMSN showed higher toxicity toward QGY-7703 hepatoma cell at all DOX concentrations used. When evaluated for antitumor efficiency, tumor inhibition ratio was found to be higher for SL-IDMSN@DOX/pDNA (96.99%) and for other combinations: SL-IDMSN/pDNA (63.39%), SLIDMSN@DOX/pGL (77.84%), and DMSN@DOX/pDNA (87.09%).

### Large pore MSN

A novel type of magnetic radial large-pore MSN with core-shell structure was fabricated for stimuli responsive *in vitro* siRNA delivery to human osteosarcoma KHOS cell line<sup>47</sup>. Initially magnetic nanocrystal clusters (MNC) were first fabricated by a hydrothermal method. Then the MNC nanoparticles were coated with a dendrimer like mesoporous silica layer by an oil/water two phase reaction method and the resulting carrier was denoted as MNC@LPMS. MNC@LPMS was functionalized with (3-Aminopropyl)-triethoxysilane (APTES) by a conventional post-grafting method and was denoted as MNC@LPMSA. In order to inhibit degradation of siRNA and prevent off target release of siRNA, MNC@LPMSA@siRNA was coated with acid labile tannic acid (TA) and the fabricated product was designated as MNC@LPMSA@siRNA@TA. After coating with TA, siRNA in MNC@LPMSA@siRNA@TA was well protected even with 20 mU RNase whereby it was almost completely degraded in MNC@LPMSA@siRNA. When evaluating the delivery capacity of MNC@LPMSA-TA system, the siRNA against polo-like kinase 1 (siPLK1) which is highly expressed in KHOS cells was used. The administration of siPLK1 via MNC@LPMSA-TA resulted cell viability of 60% compared to the untreated cells. When magnetic field was applied, the cell viability after treatment with MNC@LPMSA@siPLK1@TA was further declined to 42%.

### Mesoporous silica nanocapsule

Wang et al.<sup>48</sup> fabricated amine functionalized PEGlated mesoporous silica nanocapsules (pMSNCs) with mesopores and hollow structure for co-delivery of T-type Ca<sup>2+</sup> channel siRNA and DOX with high loading efficiency to increase sensitivity of drug-resistant breast cancer cells towards DOX. The release of DOX was found to be pH dependent

and more DOX was released at pH of 5 than 7.4. In vivo antitumor effect was evaluated in mice after MCF-7/ADR tumor reached size of  $\sim 100 \text{ mm}^3$ . The mice were treated with saline (control), free DOX, pMSNC/DOX, pMSNC/siRNA and pMSNC/DOX/siRNA at  $5 \text{ mg kg}^{-1}$  DOX and  $0.25 \text{ mg kg}^{-1}$  siRNA *via* intratumoral administration. The treatment was repeated every 4 days until the 40<sup>th</sup> day. During the 40 days treatment period no obvious body weight differences were observed among the control, pMSNC/DOX, pMSNC/siRNA and pMSNC/DOX/siRNA groups. Tumor sizes for the control group increased rapidly, and the tumor growth in the free DOX group was slightly suppressed. At the end of therapy tumor inhibition rate of free DOX, pMSNC/siRNA, pMSNC/DOX and pMSNC/DOX/siRNA was 29.8%, 47%, 45.5%, and 76%, respectively.

### Multifunctional MSN

In another study alginate-chitosan coated super-paramagnetic mesoporous silica nanoparticles (M-MSN) carrying DOX, chlorin e6 (Ce6, a photosensitizer) and shRNA against p-gp was synthesized as theranostics<sup>49</sup>. DOX and Ce6 were entrapped in the mesoporous channel (M-MSN(Dox/Ce6)). Polyelectrolyte multilayer alginate/chitosan (ALG/CHI) were deposited alternately on the surface of M-MSN(Dox/Ce6) via layer-by-layer technique. The ALG/CHI multilayer deposited on the surface of M-MSN(Dox/Ce6) offered two advantages. It acts as pH-sensitive gatekeeper for ensuring the release of drug molecules in acidic conditions and provides better biocompatibility and electrostatic absorption for shRNA. When the multilayer swells, porous structure or local defect occurs and facilitates the permeation of drug molecules<sup>49</sup>. When evaluated for breast cancer drug resistance modifying efficacy against mouse breast cancer cell EMT-6, mice in the M-MSN (Dox/Ce6)/PEM/P-gp shRNA group with laser irradiation achieved significant tumor ablation.

A study by Shi et al.<sup>50</sup> was focused to co-deliver TH287 (MutT homolog 1 inhibitor) and MDR1 siRNA against multi-drug resistant protein-1 (p-glycoprotein 1) in CAL27 tumor cells in mice. Hyaluronic acid (HA) was coated on the surface of positively charged MSN to offer three purposes: i) barrier function for the drug release from pores of MSN, ii) protect degradation of siRNA in blood, and iii) act as targeting ligand to cancer cells. The antitumor efficacy was evaluated against  $50\text{-}80 \text{ mm}^3$  CAL27 tumor cells in mice by injecting blank nanoparticles, free TH287, siRNA-TH287-MSN and HA-siRNA-TH287-MSN. At the end of treatment the volume of tumor for blank nanoparticles, free TH287, siRNA-TH287-MSN and HA-siRNA-TH287-MSN were about  $1,600 \text{ mm}^3$ ,  $1,200 \text{ mm}^3$ ,  $800 \text{ mm}^3$ , and  $400 \text{ mm}^3$ , respectively. The improved cellular uptake and controlled release of therapeutics from HA-siRNA-TH287-MSN was ascribed for better antitumor effect of HA-siRNA-TH287-MSN than siRNA-TH287-MSN.

### CONCLUSION

Synthesis of MSN have been focusing on increasing loading efficiency and sustained release of the antigens and gene materials which correlates well with enhanced therapeutic effect of the therapeutics. One technique of improving loading efficiency is by synthesis of large mesoporous MSN such as large pore MSN, HMSN, and

dendritic MSN which can simultaneously load biomolecules with synergistic effect. Premature release of loads could be prevented through coating of MSN by liposomes, alginate/chitosan blend, cyclodextrin, etc. Synthesis of MSN with doped elements showed improved degradation and therapeutic effects. Adjuvant potential of MSN in vaccine formulations is encouraging even compared to conventional adjuvants and efforts should be made to translate its clinical advantages.

### ACKNOWLEDGMENTS: NONE

### CONFLICT OF INTEREST: NONE

### REFERENCES

1. Kresge CT, Leonowicz ME, Roth WJ, Vartuli, JC, Beck JS. Ordered mesoporous molecular sieves synthesized by liquid crystal template mechanism. *Nature*.1992; 359:710-2.
2. Galarneau A, Cambon H, Di Renzo F, Ryoo R, Choi M, Fajula F. Microporosity and connections between pores in SBA-15 mesostructured silicas as a function of the temperature of synthesis. *New Journal of Chemistry*. 2003; 27(1):73-9.
3. Ballem MA, Córdoba JM, Odén M. Influence of synthesis temperature on morphology of SBA-16 mesoporous materials with a three-dimensional pore system. *Microporous and Mesoporous Materials*. 2010; 129(1-2):106-11.
4. Meleñdez-Ortiz HI, Garcí'a-Cerda LA, Olivares-Maldonado Y, Castruita G, Mercado-Silva JA, Perera-Mercado YS. Preparation of spherical MCM-41 molecular sieve at room temperature: Influence of the synthesis conditions in the structural properties. *Ceramics International*. 2012; 38(8):6353-8.
5. Mahony D, Cavallaro AS, Stahr F, Mahony TJ, Qiao SZ, Mitter N. Mesoporous silica nanoparticles act as a self-adjuvant for ovalbumin model antigen in mice. *Small*. 2013; 9(18):3138-46.
6. Zhang H, Cheng T, Lai L, Deng S, Yu R, Qiu L, Zhou J, Lu G, Zhi C, Chen J. BN nanospheres functionalized with mesoporous silica for enhancing CpG oligodeoxynucleotide mediated cancer immunotherapy. *Nanoscale*. 2018; 10(30):14516-24.
7. Yang Y, Jambhrunkar M, Abbaraju PL, Yu M, Zhang M, Yu C. Understanding the effect of surface chemistry of mesoporous silica nanorods on their vaccine adjuvant potency. *Advanced Healthcare Materials*. 2017; 6(17)
8. Wang X, Li X, Ito A, Sogo Y, Watanabe Y, Hashimoto K, Yamazaki A, Ohno T, Tsuji NM. Synergistic effects of stellated fibrous mesoporous silica and synthetic dsRNA analogues for cancer immunotherapy. *Chemical Communications*. 2018; 54 (9):1057-60.
9. Tao C, Zhu Y, Xu Y, Zhu M, Morita H, Hanagata N. Mesoporous silica nanoparticles for enhancing the delivery efficiency of immunostimulatory DNA drugs. *Dalton Transaction*.2014; 43(13):5142-50.
10. Cha BG, Jeong JH, Kim J. Extra-large pore mesoporous silica nanoparticles enabling co-delivery of high amounts of protein antigen and toll-like receptor 9 agonist for enhanced cancer vaccine efficacy. *ACS Central. Science*. 2018; 4 (4):484-92.
11. Kwon D, Cha BG, Cho Y, Min J, Park EB, Kang SJ, Kim J. Extra-large pore mesoporous silica nanoparticles for directing in vivo m2 macrophage polarization by delivering IL-4. *Nano Letters*. 2017; 17(5):2747-56.
12. Ong C, Cha BG, Kim J. Mesoporous silica nanoparticles doped with gold nanoparticles for combined cancer immunotherapy and photothermal therapy. *ACS Applied Bio Materials*. 2019; 2(8):3630-38.
13. Wang X, Li X, Ito A, Yoshiyuki K, Sogo Y, Watanabe Y, Yamazaki A, Ohno T, Tsuji NM. Hollow structure improved anti-cancer immunity of mesoporous silica nanospheres in vivo. *Small*. 2016; 12(26):3510-15.
14. Teng ZG, Su XD, Zheng YY, Sun J, Chen GT, Tian CC, Wang JD, Li H, Zhao YN, Lu GM. Mesoporous silica hollow spheres with ordered radial mesochannels by a spontaneous self-transformation approach. *Chemistry of Materials*. 2013; 25(1):98-105.
15. Xie J, Yang C, Liu Q, Li J, Liang R, Shen C, Zhang Y, Wang K, Liu L, Shezad K, Sullivan M, Xu Y, Shen G, Tao J, Zhu J, Zhang Z. Encapsulation of Hydrophilic and Hydrophobic Peptides into Hollow Mesoporous Silica Nanoparticles for Enhancement of Antitumor Immune Response. *Small*.2017; 13(40).
16. Tu J, Du G, Reza Nejadnik M, Mönkäre J, van der Maaden K, Bomans PHH, Sommerdijk NAJM, Slütter B, Jiskoot W, Bouwstra JA, Kros A. Mesoporous silica nanoparticle-coated microneedle

- arrays for intradermal antigen delivery. *Pharmaceutical Research*. 2017; 34(8):1693–1706.
17. Kong M, Tang J, Qiao Q, Wu T, Qi Y, Tan S, Gao X, Zhang Z. Biodegradable hollow mesoporous silica nanoparticles for regulating tumor microenvironment and enhancing antitumor efficiency. *Theranostics*. 2017; 7(13):3276–92.
  18. Lu Y, Yang Y, Gu Z, Zhang J, Song H, Xiang G, Yu C. Glutathione-depletion mesoporous organosilica nanoparticles as a self-adjunct and co-delivery platform for enhanced cancer immunotherapy. *Biomaterials*. 2018; 175:82–92.
  19. Abbaraju PL, Yang Y, Yu M, Fu J, Xu C, Yu C. Core-shell-structured dendritic mesoporous silica nanoparticles for combined photodynamic therapy and antibody delivery. *Chemistry-An Asian Journal*. 2017; 12(13):1465–69.
  20. Abbaraju PL, Meka AK, Song H, Yang Y, Jambhrunkar M, Zhang J, Xu C, Yu M, Yu C. Asymmetric silica nanoparticles with tunable head–tail structures enhance hemocompatibility and maturation of immune cells. *J. Am. Chem. Soc.* 2017; 139(18):6321–28.
  21. Yang Y, Lu Y, Abbaraju PL, Zhang J, Zhang M, Xiang G, Yu C. Multi-shelled dendritic mesoporous organosilica hollow spheres: roles of composition and architecture in cancer immunotherapy. *Angew. Chem. Int. Ed.*, 2017; 56(29):8446–50.
  22. Virginio VG, Bandeira NC, dos Anjos Leal FM, Lancellotti M, Zaha A, Ferreira HB. Assessment of the adjuvant activity of mesoporous silica nanoparticles in recombinant *Mycoplasma hypopneumoniae* antigen vaccines. *Heliyon*. 2017; 3(1):e00225.
  23. Wang X, Li X, Yoshiyuki K, Watanabe Y, Sogo Y, Ohno T, Tsuji NM, Ito A. Comprehensive mechanism analysis of mesoporous-silica-nanoparticle-induced cancer immunotherapy. *Advanced Healthcare Materials*. 2016; 5(10):1169–76.
  24. Wang X, Li X, Ito A, Sogo Y, Watanabe Y, Tsuji NM, Ohno T. Biodegradable metal ions doped mesoporous silica nanospheres stimulate anti-cancer th1 immune response *in vivo*. *ACS Applied Materials & Interfaces*. 2017; 9(50):43538–44.
  25. Mahony D, Mody KT, Cavallaro AS, Hu Q, Mahony TJ, Qiao S, Mitter N. Immunisation of sheep with bovine viral diarrhoea virus, E2 protein using a freeze-dried hollow silica mesoporous nanoparticle formulation. *PLoS One*. 2015; 10(11):e0141870.
  26. Bai M, Dong H, Su X, Jin Y, Sun S, Zhang Y, Yang Y, Guo H. Hollow mesoporous silica nanoparticles as delivery vehicle of foot-and-mouth disease virus-like particles induce persistent immune responses in guinea pigs. *Journal of Medical Virology*, 91(6):941–8.
  27. Ding B, Shao S, Yu C, Teng B, Wang M, Cheng Z, Wong KL, Ma P, Lin J. Large-pore mesoporous-silica-coated upconversion nanoparticles as multifunctional immunoadjuvants with ultrahigh photosensitizer and antigen loading efficiency for improved cancer photodynamic immunotherapy. *Advanced Materials*. 2018; 30(52).
  28. Peng X, Liang Y, Yin Y, Liao H, Li L. Development of a hollow mesoporous silica nanoparticles vaccine to protect against house dust mite induced allergic inflammation. *International Journal of Pharmaceutics*. 2018; 549(1–2):115–123.
  29. Wang D, Xu X, Zhang K, Sun B, Wang L, Meng L, Liu Q, Zheng C, Yang B, Sun H. Co-delivery of doxorubicin and MDR1-siRNA by mesoporous silica nanoparticles-polymer polyethylenimine to improve oral squamous carcinoma treatment. *International Journal of Nanomedicine*. 2018; 13:187–98.
  30. Zhan Z, Zhang X, Huang J, Huang Y, Huang Z, Pan X, Quan G, Liu H, Wang L, Wu C. Improved gene transfer with functionalized hollow mesoporous silica nanoparticles of reduced cytotoxicity. *Materials*. 2017; 10(7):731.
  31. Chang JH, Tsai PH, Chen W, Chiou SH, Mou CY. Dual delivery of siRNA and plasmid dna using mesoporous silica nanoparticles to differentiate induced pluripotent stem cells into dopaminergic Neurons. *Journal of Materials Chemistry B*. 2017; 5(16):3012–23.
  32. Mahmoodi M, Behzad-Behbahani A, Sharifzadeh S, Abolmaali SS, Tamaddon AM. Co-condensation synthesis of well-defined mesoporous silica nanoparticles: effect of surface chemical modification on plasmid DNA condensation and transfection. *IET Nanobiotechnology*. 2017; 11(8):995–1004.
  33. Chen L, She X, Wang T, Shigdar S, Duan W, Kong L. Mesoporous silica nanorods toward efficient loading and intracellular delivery of siRNA. *Journal of Nanoparticle Research*. 2018; 20 (37).
  34. Sun L, Wang D, Chen Y, Wang L, Huang P, Li Y, Liu Z, Yao H, Shi J. Core-shell hierarchical mesostructured silica nanoparticles for gene/chemo-synergistic stepwise therapy of multidrug-resistant cancer. *Biomaterials*. 2017; 133:219–228.
  35. Dilnawaz F, Sahoo SK. Augmented anticancer efficacy by si-RNA complexed drug loaded mesoporous silica nanoparticles in lung cancer therapy. *ACS Applied Nano Materials*, 2018; 1(2):730–40.
  36. Roberts CM, Shahin SA, Wen W, Finlay JB, Dong J, Wang R, Dellinger TH, Zink JI, Tamaño F, Glackin CA. Nanoparticle delivery of siRNA against TWIST to reduce drug resistance and tumor growth in ovarian cancer models. *Nanomedicine: Nanotechnology, Biology, and Medicine*. 2016; 13(3):965–76.
  37. Terauchi M, Kajiyama H, Yamashita M, Kato M, Tsukamoto H, Umezū T, Hosono S, Yamamoto E, Shibata K, Ino K, Nawa A, Nagasaka T, Kikkawa F. Possible involvement of TWIST in enhanced peritoneal metastasis of epithelial ovarian carcinoma. *Clinical & Experimental Metastasis*. 2007; 24(5):329–39.
  38. Yang J, Mani SA, Donaher JL, Ramaswamy S, Itzykson RA, Come C, Savagner P, Gitelman I, Richardson A, Weinberg RA. Twist, a master regulator of morphogenesis, plays an essential role in tumor metastasis. *Cell*. 2004; 117(7):927–39.
  39. Shen J, Liu H, Mu C, Wolfram J, Zhang W, Kim HC, Zhu G, Hu Z, Ji LN, Liu X, Ferrari M, Mao ZW, Shen H. Multi-step encapsulation of chemotherapy and gene silencing agents in functionalized mesoporous silica nanoparticles. *Nanoscale*, 2017; 9(16):5329–41.
  40. Li Y, Duo Y, Bi J, Zeng X, Mei L, Bao S, He L, Shan A, Zhang Y, Yu X. Targeted delivery of anti-miR-155 by functionalized mesoporous silica nanoparticles for colorectal cancer therapy. *International Journal of Nanomedicine* 2018; 13:1241–56.
  41. Jiang S, Zhang HW, Lu MH, He XH, Li Y, Gu H, Liu MF, Wang ED. MicroRNA-155 functions as an OncomiR in breast cancer by targeting the suppressor of cytokine signaling 1 gene. *Cancer Research*. 2010; 70(8):3119–27.
  42. Wang S, Liu Z, Wang L, Zhang X. NF- $\kappa$ B signaling pathway, inflammation and colorectal cancer. *Cellular and Molecular Immunology*. 2009; 6(5):327–34.
  43. Ben-Neriah Y, Karin M. Inflammation meets cancer, with NF- $\kappa$ B as the match maker. *Nature Immunology*. 2011; 12(8):715–23.
  44. Lin JT, Liu ZK, Zhu QL, Rong XH, Liang CL, Wang J, Ma D, Sund J, Wang GH. Redox-responsive nanocarriers for drug and gene co-delivery based on chitosan derivatives modified mesoporous silica nanoparticles. *Colloids and Surfaces B: Biointerfaces*, 2017; 155:41–50.
  45. Wang Y, Song H, Yu M, Xu C, Liu Y, Tang J, Yang Y, Yu C. Room temperature synthesis of dendritic mesoporous silica nanoparticles with small sizes and enhanced mRNA delivery performance. *Journal of Materials Chemistry B*. 2018; 6(24):4089–95.
  46. Li Z, Zhang L, Tang C, Yin C. Co-delivery of doxorubicin and survivin shRNA-expressing plasmid via microenvironment-responsive dendritic mesoporous silica nanoparticles for synergistic cancer therapy. *Pharmaceutical Research*. 2017; 34(12):2829–41.
  47. Xiong L, Bi J, Tang Y, Qiao SZ. Magnetic Core-shell silica nanoparticles with large radial mesopores for siRNA delivery. *Small*, 2016; 12(34):4735–42.
  48. Wang S, Liu X, Chen S, Liu Z, Zhang X, Liang XJ, Li L. Regulation of Ca<sup>2+</sup> signaling for drug-resistant breast cancer therapy with mesoporous silica nanocapsules encapsulated doxorubicin/siRNA cocktail. *ACS Nano*. 2018; 13(1):274–83.
  49. Yang H, Chen Y, Chen Z, Geng Y, Xie X, Shen X, Li T, Li S, Wu C, Liu Y. Chemo-photodynamic combined gene therapy and dual-modal cancer imaging achieved by pH responsive alginate/chitosan multilayer-modified magnetic mesoporous silica nanocomposites. *Biomaterials Science*, 2017; 5(5):1001–13.
  50. Shi XL, Li Y, Zhao LM, Su LW, Ding G. Delivery of MTH1 inhibitor (TH287) and MDR1 siRNA via hyaluronic acid-based mesoporous silica nanoparticles for oral cancers treatment. *Colloids and Surfaces B: Biointerfaces*, 173:599–606.